This structural change may also account for the slight aberration in the trend in $\Delta S°'$ values which occurs at this point.

The observation that the open-chain ligand complex Cu(Me_2-2,3,2-S_4) exhibits a $\Delta H°'$ value which is identical with that for the complex with the 14-ane-S_4 ligand illustrates the fallacy in the earlier claim[4] that such cyclic ligand species would form stronger coordinate bonds than would their open-chain counterparts. In fact, the difference in $\Delta H°'$ values for the Me_2- and Et_2-2,3,2-S_4 complexes reflects the fact that the ethyl groups in the latter complex encounter steric problems, resulting in a slightly nonplanar coordination of one terminal sulfur donor atom as revealed in the resolved crystal structure.[14,19]

A comparison of the thermodynamic values exhibited by the Cu(II) complexes with 15-ane-S_4 and 15-ane-S_5 is also of interest. The latter ligand bonds all five sulfur donors to the Cu(II) ion, resulting in greater internal strain within the complexed ligand. This may account for the reasonably constant $\Delta H°$ value for the two complexes despite the extra Cu-S bond formed with the pentathia ether ligand. The significantly larger $\Delta S°$ value for the latter ligand is contrary to the greater rigidity experienced by this ligand upon complexation and is clearly a reflection of the entropy contribution resulting from complete desolvation of Cu(II) in this complex.

Conclusions

The following general conclusions are consistent with the experimentally evaluated stability constant values for the Cu^{II}-polythia ether complexes.

(1) Increasing the concentration of $HClO_4$ in the solvent medium results in a marked increase in the apparent stability constant values for the Cu^{II}-polythia ether complexes. As evaluated for Cu^{II}(14-ane-S_4) in aqueous solution, the increase in the apparent stability constant at 25 °C amounts to approximately 2-fold, 5-fold, and 17-fold for solutions containing 0.10, 0.50, and 1.00 M $HClO_4$, respectively. This stability constant increase is consistent with a model in which perchlorate ion forms a tight ion pair (or a ternary complex) with the Cu^{II}-polythia ether complexes for which the 25 °C activity equilibrium constant value is 24 M^{-1}.

(2) With the assumption that the perchlorate ion effect is roughly equivalent for all of the Cu^{II}-polythia ethers studied, the entropy of complex formation is seen to steadily decrease as the ring size of the ligand increases from 12-ane-S_4 ($\Delta S°$ = +15.9 eu) to the open-chain species ($\Delta S°$ = -5.4 and -2.5 eu) with a slight discontinuity for 16-ane-S_4. The fact that the maximum stability occurs with the 14-ane-S_4 ligand complex is attributable to the overriding favorable enthalpy which correlates to the optimal coordination geometry (shortest Cu-S bond lengths combined with planar coordination as revealed from crystallographic studies.

(3) The value of $\Delta H°$ for the open-chain ligand complexes is virtually identical with that obtained for the complex involving the optimally fitting cyclic ligand 14-ane-S_4. Thus, the *macrocyclic effect* is wholly attributable to the *more favorable entropy* associated with the less flexible cyclic ligand.

Acknowledgment. This work was supported by the National Institute of General Medical Sciences under Grant GM-20424.

Registry No. Cu, 7440-50-8; $HClO_4$, 7601-90-3; 12-ane-S_4, 25423-56-7; 13-ane-S_4, 25423-54-5; 14-ane-S_4, 24194-61-4; 15-ane-S_4, 57704-75-3; 16-ane-S_4, 295-91-0; 15-ane-S_5, 36338-04-2; Me_2-2,3,2-S_4, 25676-65-7; Et_2-2,3,2-S_4, 57704-77-5.

Contribution from the Chemistry Department, University of Houston, Houston, Texas 77004, and the Department of Chemistry, University of Iowa, Iowa City, Iowa 52242

Electrochemical and NMR Studies of Six-Coordinate Oxidized μ-Nitrido Iron Porphyrin Dimers

KARL M. KADISH,*[1] RATHBUN K. RHODES,[1] LAWRENCE A. BOTTOMLEY,[1] and HAROLD M. GOFF*[2]

Received April 13, 1981

The reaction of μ-nitrido-bis[(5,10,15,20-tetraphenylporphyrinato)iron] cation with aniline and 11 substituted pyridines in the solvent 1,2-dichloroethane was studied electrochemically. Half-wave potential shifts as a function of added ligand concentration indicated that bisligated adducts of the oxidized μ-nitrido dimer were formed in solution. For the ligands investigated, the magnitude of the formation constants ranged from $10^{3.8}$ to $10^{8.6}$. A plot of log β_2 vs. pK_a of the added ligand suggests that σ bonding is the predominant mode of ligand to metal interaction. A common dimeric product is produced by either one-electron chemical or electrochemical oxidation of the parent μ-nitrido complex. Nuclear magnetic resonance spectroscopy has been utilized to characterize the oxidized product. Bisligation of nitrogenous bases to the oxidized dimeric product has been unequivocally demonstrated. Tentative evidence for monoligation at low temperatures is presented.

Introduction

The synthesis[3] as well as the molecular structure[4] of μ-nitrido-bis[(5,10,15,20-tetraphenylporphyrinato)iron], (TPP-Fe)$_2$N, has been recently reported. Comparisons of the physical properties of this complex with similar compounds were difficult as this was the first example of two first-row transition-metal atoms being bridged with a single nitrogen atom. Other dimeric μ-nitrido species have been reported,[5] but these complexes contain second- and third-row transition metals. Recently, we have reported XPS results[6] which are consistent with the presence of two equivalent, *low-spin* iron atoms in this dimer. This would be only the second case[7] of a five-coordinate iron porphyrin complex given the low-spin

(1) University of Houston.
(2) University of Iowa.
(3) Summerville, D. A.; Cohen, I. A. *J. Am. Chem. Soc.* **1976**, *98*, 1747.
(4) Scheidt, W. R.; Summerville, D. A.; Cohen, I. A. *J. Am. Chem. Soc.* **1976**, *98*, 6623.
(5) Griffith, W. P. *Coord. Chem. Rev.* **1972**, *8*, 369.
(6) Kadish, K. M.; Bottomley, L. A.; Brace, J. G.; Winograd, N. *J. Am. Chem. Soc.* **1980**, *102*, 4341.
(7) Scheidt, W. R.; Frisse, M. E. *J. Am. Chem. Soc.* **1975**, *97*, 17.

0020-1669/81/1320-3195$01.25/0

assignment. On the basis of similarity of resonance Raman bands, the μ-nitrido dimer has been formulated as having a high-spin state much as is the case for the μ-oxo iron(III) porphyrin dimer.[8]

A recent electrochemical investigation by Kadish and coworkers[9] has demonstrated that the neutral [TPPFe$^{III^1/_2}$–N–Fe$^{III^1/_2}$TPP] dimer can be reversibly oxidized to form the cationic [TPPFe^{IV}–N–Fe^{IV}TPP]$^+$ dimer or reduced in a one-electron transfer to form [TPPFe^{III}–N–Fe^{III}TPP]$^-$, which is isoelectronic with the μ-oxo dimer. The potentials for reduction of the parent dimer were essentially invariant in the solvent systems investigated. However, the potential for the electrogeneration of $[(TPPFe)_2N]^+$ in pyridine was 410 mV more cathodic than the potential measured in CH_2Cl_2 for the same electron-transfer step.[10] One explanation for this potential shift was that pyridine was complexing with the μ-nitrido dimer or the oxidized product. This was an intriguing possibility, as the μ-oxo dimer is known not to coordinate any additional ligands. To account for the observed potential difference, as well as to prove or disprove axial ligand coordination by pyridine, an intensive electrochemical investigation of the reactivity of the μ-nitrido dimer was undertaken. Complementary NMR work was performed to further elucidate molecular structures and chemical equilibria. This paper presents voltammetric, spectroelectrochemical, and NMR evidence for the existence of a complexed μ-nitrido dimer in which the coordination sphere about each iron atom may be filled. Formation constants for the addition of aniline and 11 substituted pyridines to $[(TPPFe)_2N]^+$ as well as electrode potentials for the redox reaction $[(TPPFeL)_2N]^+ \overset{e^-}{\rightleftharpoons} [(TPPFe)_2N]^0 + 2L$ are reported.

Experimental Section

$(TPPFe)_2N$ was the gracious gift of Professor Irwin A. Cohen. The supporting electrolyte, tetrabutylammonium perchlorate (Eastman) (TBAP), was recrystallized from ethyl acetate and then dried in vacuo at 80 °C prior to use. Dichloroethane ($EtCl_2$) was purchased from Mallinckrodt. Prior to use, portions were extracted with equal volumes of concentrated H_2SO_4, distilled H_2O, and a 5% aqueous KOH solution. The extract was then distilled from P_2O_5 and stored in the dark over activated 4-Å molecular sieves. Deuterated chloroform was washed with aqueous K_2CO_3 solution, dried over $CaCl_2$, distilled, and stored over activated molecular sieves. Pyridine was purchased from Fisher Scientific. It was distilled from CaO under N_2 and stored over 4-Å molecular sieves. All other ligands used in this study were purchased from Aldrich Chemicals and, unless noted, were used as received. 3-Picoline and 4-picoline were distilled from KOH pellets and were stored in the dark over 4-Å molecular sieves. 3-Cyanopyridine, and 4-cyanopyridine were recrystallized from benzene and dried in vacuo at ambient temperature. The electrochemical equipment and experimental details were identical with those previously described.[11] All potentials were measured as $E_{1/2} = (E_{p,a} + E_{p,c})/2$ from cyclic voltammetric data and are reported vs. the SCE. Nuclear magnetic resonance spectra were recorded with a multinuclear JEOL FX-90Q instrument.

Results

Electrochemical Measurements. A typical cyclic voltammogram $[(TPPFe)_2N]^0$ in $EtCl_2$ is shown in Figure 1a. Two separate electron transfer processes are observed at $E_{1/2}$ = +0.17 and −1.19 V *vs.* SCE. Variable-scan-rate data between 0.02 and 10.0 V/s indicates that $i_{p/v}^{1/2}$ is constant and that $i_{p,a}/i_{p,c}$ is equal to unity. Although $E_{p,c} - E_{p,a}$ is somewhat larger than the theoretical value of 60 mV for a reversible one-electron transfer, thin-layer coulometric results confirm the chemical reversibility of each one-electron process. Figure

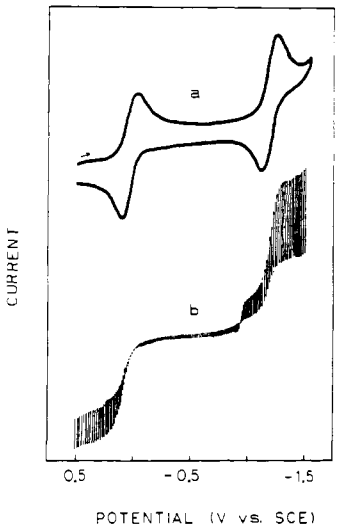

Figure 1. Typical voltammogram of 1.0 mM $(TPPFe)_2N$ in $EtCl_2$, 0.1 M TBAP: (a) cyclic voltammogram at Pt electrode (scan rate 0.50 V/s); (b) polarogram at DME (scan rate 0.02 V/s, t = 0.5 s).

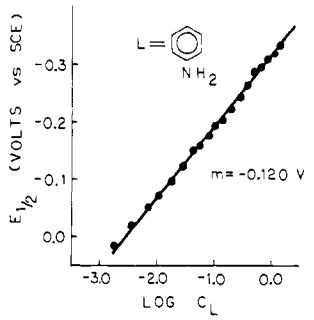

Figure 2. Half-wave potential dependence on the concentration of aniline added to solutions of 1.0 mM $(TPPFe)_2N$ in $EtCl_2$, 0.1 M TBAP.

1b depicts a typical polarogram obtained for the solution used in the cyclic voltammetric experiments. It shows, quite convincingly, that the quasireversible one-electron process at +0.17 V is an oxidation and that the process at −1.19 V is a reduction.

Additions of aliquots of aniline produced negative shifts in potential for the oxidation of $[(TPPFe)_2N]^0$. This is shown in Figure 2. In contrast, potentials for the reduction of $[(TPPFe)_2N]^0$ were invariant over the ligand concentration range studied. The potential shifts observed were consistent with complexation of the oxidized material, $[(TPPFe)_2N]^+$, by two aniline molecules but not of the starting material. Similar results were obtained for addition of 11 substituted pyridines. Although NMR results indicate the probable existence of a monoligated adduct at high dimer and low pyridine concentrations (vide infra), only bisadduct formation was observed electrochemically. Comparison of the potential shifts with added ligand to those previously presented for monomeric TPPFeX[11] confirms the assignment of a six-coordinate μ-nitrido dimer. From the potential shifts observed, formation constants for the addition of two molecules per dimer were calculated according to eq 1. These results are presented

$$[(TPPFe)_2N]^+ + 2L \rightleftarrows [(TPPFeL)_2N]^+ \qquad (1)$$

in Table I. Also given are half-wave potentials for the reduction of $[(TPPFe)_2N]^+$ and $[(TPPFeL)_2N]^+$, at 1.0 M [ligand]. The method of calculation is identical with that previously described.[11]

Electronic Spectra. Thin-layer spectroelectrochemical data in support of the electrochemical results are presented in Figure 3. The detail of the visible and Soret bands observed in either

(8) Schick, G. A.; Bocian, D. F. *J. Am. Chem. Soc.* **1980**, *102*, 7982.
(9) Kadish, K. M.; Cheng, J. S.; Cohen, I. A.; Summerville, D. A. *ACS Symp. Ser.* **1977**, *No. 38*, Chapter 5.
(10) This reaction was erroneously reported in ref 9 as a reduction.
(11) Kadish, K. M.; Bottomley, L. A. *Inorg. Chem.* **1980**, *19*, 832.

Table I. Formation Constants for the Addition of Selected Ligands to $(TPPFe)_2N$

ligands	σ^a	pK_a^b	$\log \beta_2^{c,d}$	$E_{1/2}$, V[e]	$\Delta E_{1/2}/\Delta \log C_L$[f]
neat $EtCl_2$				+0.17	
3,5-dichloropyridine	0.75	0.67	3.8 ± 0.2	−0.06	−118
3-cyanopyridine	0.56	1.45	4.35 ± 0.2	−0.10	−106
4-cyanopyridine	0.66	1.86	4.74 ± 0.15	−0.12	−119
3-chloropyridine	0.37	2.81	5.8 ± 0.2	−0.17	−116
3-bromopyridine	0.39	2.84	5.6 ± 0.1	−0.16	−112
3-acetylpyridine	0.38	3.18	6.90 ± 0.17	−0.24	−122
4-acetylpyridine	0.50	3.51	6.65 ± 0.25	−0.22	−116
aniline		4.63	6.89 ± 0.12	−0.24	−120
pyridine	0.00	5.29	7.62 ± 0.04	−0.28	−120
3-picoline	−0.07	5.79	7.8 ± 0.2	−0.30	−117
4-picoline	−0.17	5.98	8.10 ± 0.09	−0.31	−120
3,4-lutidine	−0.24	6.46	8.6 ± 0.2	−0.34	−118

[a] Taken from: Gordon, A. J.; Ford, R. A. "The Chemist's Companion"; Wiley: New York, 1972; pp 144–147. [b] Taken from: from Schoefield, K. "Hetero-Aromatic Nitrogen Compounds"; Plenum Press: New York, 1967; p 146. [c] Measured in $EtCl_2$, 0.1 M TBAP. [d] Temperature = 23 ± 2 °C. [e] Measured at 1.0 M ligand concentration and reported vs. the SCE. [f] Slope of $E_{1/2}$ vs. log C_L trace listed in mV. See Figure 2 for the actual plot obtained for addition of aniline.

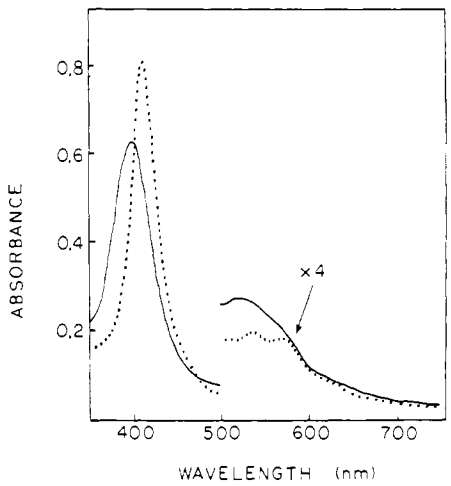

Figure 3. Spectra of 5×10^{-4} M $[(TPPFe)_2N]^+$, 0.20 M TBAP in (a) $EtCl_2$ (—) and (b) pyridine (···). Path length is 0.12 mm.

$EtCl_2$ or pyridine does not resemble previously reported spectra for porphyrin cation radicals.[12] The spectrum of $[(TPPFe)_2N]^+$ is more like those reported by Felton et al.[13,14] for oxidized $[(TPPFe)_2O]$ species in that the Soret band is broad and distinctive visible bands are absent. Thus, oxidation of the parent $[TPPFe^{IV}–N–Fe^{III}TPP]$ dimer involves either removal of an electron from the bridging atom formally yielding a $[TPPFe^{IV}–N^{-II}–Fe^{III}TPP]^+$ species or removal of an electron from the iron(III) center yielding a $[TPPFe^{IV}–N^{-III}–Fe^{IV}TPP]^+$ species. The spectral differences observed when dimer is dissolved in $EtCl_2$ and pyridine (Figure 3a vs. b) are too large to be attributed only to differences in nonspecific solute–solvent interactions. Direct coordination of the dimer by pyridine is indicated. Comparison of the well-known $[TPPFe(L_2)]^+$ spectra[15] with that presented in Figure 3b provides additional proof that the oxidized material is a coordinated dimeric species.

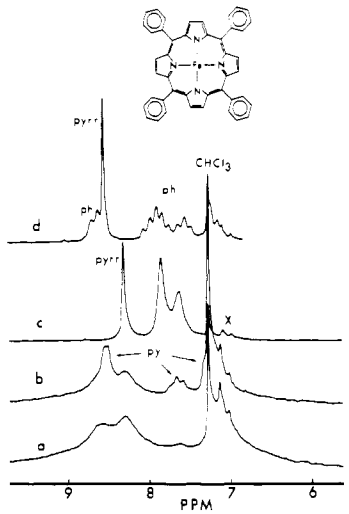

Figure 4. Proton NMR spectra of μ-nitrido dimer species ($CDCl_3$ solvent, 26 °C, 5 mM [dimer], referenced to Me_4Si): (a) $(TPPFe)_2N$; (b) $(TPPFe)_2N$ with 10 mM pyridine; (c) $[(TPPFe)_2N]^+$ generated by addition of one-electron equivalent of I_2/Ag^+; (d) $[(TPPFe)_2N]^+$ with 15 mM pyridine. (The × signals are from xylene of solvation.)

Both $[(TPPFe)_2N]^+$ and the pyridine-ligated species may be generated through chemical oxidation. Thus, a spectrum identical with that of Figure 3a is obtained in chloroform or methylene chloride solution upon addition of one-electron equivalent per dimer unit of molecular iodine (dissolved in chloroform) and 1 equiv of silver perchlorate (dissolved in acetone). This I_2/Ag^+ combination has proven to be a powerful and convenient oxidizing agent in other metalloporphyrin redox studies.[16] Addition of excess pyridine to the $[(TPPFe)_2N]^+$ solution yields a spectrum identical with that recorded in a thin-layer electrochemical cell in Figure 3b. Iodine alone will oxidize $(TPPFe)_2N$, but an excess is required. In the presence of pyridine, however, one-electron equivalent of I_2 oxidizes $(TPPFe)_2N$ to yield the bis-ligated spectrum of Figure 3b.

NMR Characterization. Nuclear magnetic resonance spectroscopy has been of unquestionable value in elucidating the electronic, magnetic, and molecular structural properties as well as dynamic and thermodynamic aspects of ligand binding in metalloporphyrins.[17] The technique has been utilized to confirm and expand on the findings reported for oxidation and subsequent ligation of $(TPPFe)_2N$. The aromatic region proton NMR spectrum of $(TPPFe)_2N$ is shown in Figure 4a. Broad overlapping signals are observed at 8.6, 8.3, and 7.6, similar to that noted earlier by Summerville and Cohen.[3] The preparation employed in this study contains xylene of crystallization as was found in the molecular structural determination.[4] Addition of 2 equiv of pyridine (Figure 4b) to the $(TPPFe)_2N$ species yields a spectrum with additional signals corresponding seemingly to those of the free, nonligated pyridine molecule. This has been confirmed by recording the carbon-13 spectrum in which well-resolved signals for free pyridine are seen. Further evidence supporting no significant affinity for pyridine binding to $(TPPFe)_2N$ is found in the deuterium NMR spectrum (with use of pyridine-d_5), in which case free pyridine signals are shifted less than 0.2 ppm.

Oxidation of $(TPPFe)_2N$ with either one-electron equivalent of I_2/Ag^+ or with excess iodine produces a substantial change in the proton NMR spectrum as may be seen in Figure 4c.

(12) Felton, R. H. In "The Porphyrins"; Dolphin, D., Ed.; Academic Press: New York, 1979; Vol. 5, Chapter 3.
(13) Felton, R. H.; Owen, G. S.; Dolphin, D.; Fajer, J. *J. Am. Chem. Soc.* **1971**, *93*, 6332.
(14) Felton, R. H.; Owen, G. S.; Dolphin, D.; Forman, A.; Borg, D. C.; Fajer, J. *Ann. N.Y. Acad. Sci.* **1973**, *206*, 504.
(15) Walker, F. A.; Lo, M.; Ree, M. T. *J. Am. Chem. Soc.* **1976**, *98*, 5552.
(16) Shine, H. J.; Padilla, A. G.; Mu, S. M. *J. Org. Chem.* **1979**, *44*, 4069.
(17) La Mar, G. N.; Walker, F. A. In "The Porphyrins"; Dolphin, D., Ed.; Academic Press: New York, 1979; Vol. 4, Chapter 2.

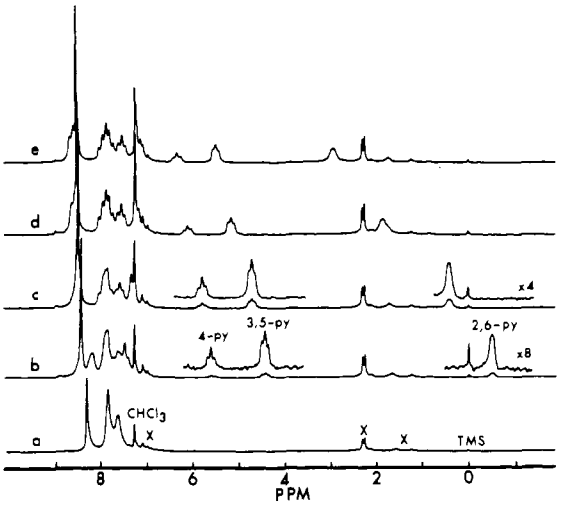

Figure 5. Pyridine titration of $[(TPPFe)_2N]^+$ ($CDCl_3$ solvent, 26 °C, 5 mM dimer, referenced to Me_4Si): (a) 0.0 mM pyridine; (b) 3.8 mM pyridine; (c) 7.5 mM pyridine; (d) 11.2 mM pyridine; (e) 15.0 mM pyridine. The × signals are from xylene of solvation, acetone, and solvent hydrocarbon impurities.

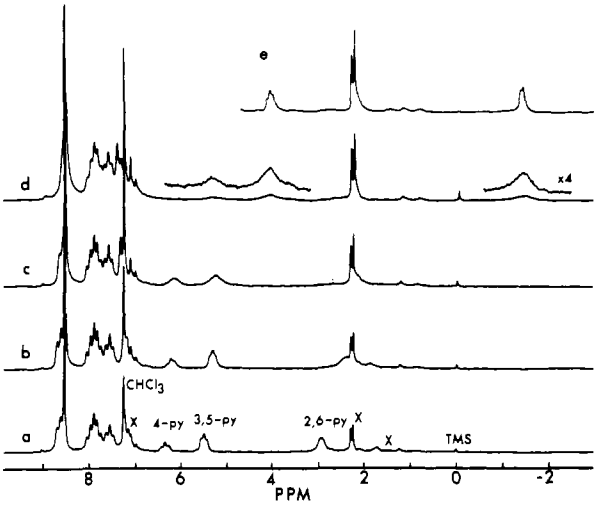

Figure 6. Variable-temperature proton NMR spectra of $[(TPPFe)_2N]^+$ (5 mM with 15 mM pyridine, $CDCl_3$ solvent, referenced to Me_4Si): (a) 26 °C; (b) 0 °C; (c) −25 °C; (d) −55 °C; (e) −77 °C (CD_2Cl_2 solvent). The × signals are from xylene of solvation, acetone, and solvent hydrocarbon impurities.

(Addition of more than one-electron equivalent of I_2/Ag^+ yields a green solution with very broad NMR signals thought to be a radical species.) The 8.32-ppm signal is assigned to the eight pyrrole protons on the basis of pyridine titrations to give the bis-ligated species (vide infra). Variable-temperature measurements from 26 to −55 °C show no changes in the spectral pattern and only small downfield shifts of 0.06, 0.01, and 0.10 ppm for the 8.32, 7.85, and 7.64 ppm resonances, respectively. Line broadening of the phenyl resonances is suggestive of weak paramagnetism in $[(TPPFe)_2N]^+$, although electron exchange with a trace contaminant of paramagnetic $(TPPFe)_2N$ or radical species cannot be ruled out. Spectral examination using a 25-kHz window revealed no detectable quantities (<5%) of high-spin iron(III) monomers, low-spin iron(III) monomers, or μ-oxo dimer in $[(TPPFe)_2N]^+$ solutions or in solutions to which pyridine was added. The equivalence of NMR samples with respect to electrochemically generated species was verified by recording the electronic spectra of solutions following NMR spectral acquisition.

Effects of excess pyridine on the porphyrin resonances of $[(TPPFe)_2N]^+$ are illustrated in Figure 4d. The pyrrole resonance is readily assigned, and phenyl signals have sharpened such that spin–spin splittings are now resolved. Overlap and possible nonequivalence of ortho and meta protons (as a consequence of slow phenyl rotation) precludes unequivocal phenyl resonance assignment until phenyl-substituted and selectively deuterated species are examined. Sequential addition of pyridine to $[(TPPFe)_2]^+$ has been carried out, and selected NMR spectra are shown in Figure 5. High-affinity binding of pyridine is clearly illustrated in Figure 5b for the condition where total ligand concentration is substoichiometric. Pyridine resonances are readily assigned based on intensity, spin–spin splittings, and expected magnitudes of ring current shifts. Ligand exchange is rapid on the NMR time scale as is evident in migration of pyridine resonances toward the normal aromatic region as the concentration of free pyridine is increased. A binding stoichiometry of greater than one pyridine per dimer unit is illustrated, for example, in spectrum 5d which contains 2.25 equiv of pyridine per dimer. In the fast exchange limit, the mole-fraction-weighted resonance would appear at 4.5 ppm if only 1 equiv was coordinated. The fact that the signal appears at 1.9 ppm is suggestive of bis ligation. Attempts to calculate β_2 from spectra b–e in Figure 5 gave results which approached the electrochemically determined β_2 but which decreased with increased pyridine concentration. The possibility of monoligation at low pyridine concentrations and high dimer concentrations may serve to explain the apparently variable β_2 values. Additional evidence for monoligation of pyridine at low temperature will be presented subsequently. It should be noted that aniline titration of $[(TPPFe)_2N]^+$ yielded NMR results essentially equivalent to those reported for pyridine. At low aniline concentrations, signals for coordinated aniline were located at 2.5 (2 protons), 6.1 (2 protons), and 5.49 ppm (1 proton). With excess aniline present, the porphyrin proton signals matched those of Figure 5e.

Variable-temperature spectra of a $[(TPPFe)_2N]^+$ solution containing 3.0 equiv of pyridine per dimer unit are shown in Figure 6. Spectra are consistent with an increased binding affinity at lower temperature and with approach of the slow exchange limit at −55 °C. At −77 °C in methylene chloride solution (Figure 6e), well-resolved coordinated pyridine resonances are seen. Integration of coordinated signal intensities at −77 °C further supports bis ligation in the presence of adequate pyridine. Observations attributable to monopyridine ligation at −77 °C have also been made. Thus, if a titration of the type shown in Figure 5 is carried out at −77 °C, a 2,6-pyridine proton resonance is seen at −1.26 ppm when small amounts of pyridine are present. With addition of 0.5 equiv per dimer, a small new signal appears at −1.46 ppm. Further addition of pyridine causes disappearance of the −1.26-ppm signal and increased intensity of the −1.46-ppm signal. With 2.0 equiv of pyridine or with excess pyridine, only the −1.46-ppm resonance is observed. The −1.26-ppm signal seemingly corresponds to a single coordinated pyridine residue, whereas the −1.46-ppm resonance results from two coordinated pyridine ligands. Serious overlap of signals in the aromatic region precludes identification of porphyrin signals belonging to the monoligated complex.

Sizeable upfield shifts for coordinated pyridine protons reflect a predominant porphyrin ring current contribution. Shift differences of −7.64[18] and −7.8 ppm[19] for the 2,6-protons of coordinated vs. free pyridine are noted for ruthenium(II) porphyrin pyridine and cobalt(III) porphyrin pyridine complexes, respectively. Proximity of a second porphyrin ring in the dimer induces an additional approximately 2-ppm upfield

(18) Eaton, S. S.; Eaton, G. R. *Inorg. Chem.* **1976**, *15*, 134.
(19) Gouedard, M.; Gaudemer, F.; Gaudemer, A. *Tetrahedron Lett.* **1973**, 2257.

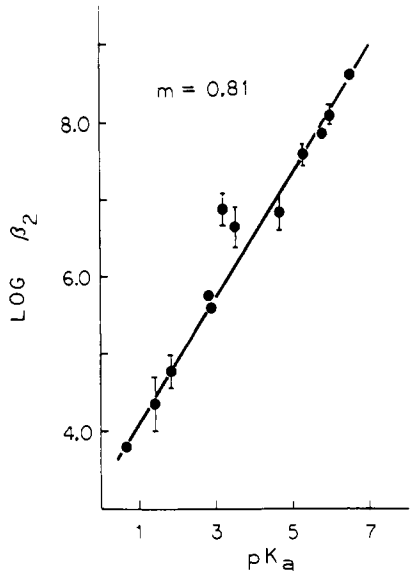

Figure 7. Dependence of $[(TPPFeL)_2N]^+$ formation constant magnitudes on ligand pK_a. See Table I for ligand identification.

shift[20] that would expectedly leave the 2,6-proton signal upfield from Me_4Si. Although ring current effects may be invoked to explain the magnitude of ligand shifts, a small contribution from weak paramagnetism or significant conformational changes is also suggested by variable-temperature measurements. For the 2,6-proton resonance of coordinated pyridine in a solution of $[(TPPFe)_2N]^+$ containing 0.5 equiv of pyridine, the following values were recorded: 26 °C, –0.63 ppm; 0 °C, –1.01 ppm; –25 °C, –1.14 ppm; –55 °C, –1.19 ppm; –77 °C, –1.26 ppm. Phenyl resonances likewise show downfield shifts of up to 0.2 ppm over this temperature range.

Solution magnetic measurements were carried out by the Evans (NMR) method.[21] A magnetic moment of 2.08 μ_B per dimer unit was determined for the parent $(TPPFe)_2N$ species with the use of the diamagnetic correction factor of -386×10^{-6} cgsu/mol for H_2TPP as reported by Summerville and Cohen.[3] The 2.08-μ_B is in excellent agreement with the solid-state measurement of 2.04 μ_B reported by these authors.[3] With the use of the now recommended diamagnetic correction of -700×10^{-6} cgsu/mol[22] a magnetic moment of 2.4 μ_B is calculated. Attempts to identify any paramagnetism in $[(TPPFe)_2N]^+$ and $[(TPPFePy)_2N]^+$ resulted in no measureable separation of the Me_4Si signal in the iron porphyrin solution and that of the reference capillary. On the basis of concentrations and expected spectral resolution, magnetic moments must be less than 1.8 μ_B (when the more recent diamagnetic correction[22] is used).

Discussion

Linear free energy relationships have been constructed equating the formation constant magnitudes with the respective electron-donating or electron-withdrawing substituents on the coordinating ligand and the pK_a of the selected pyridine. Increasing the pK_a of the substituted pyridine substantially increases the magnitude of β_2 as listed in Table I and plotted in Figure 7. This suggests that σ bonding is the predominant mode of ligand to metal interaction. Comparison of the log β_2 for aniline (6.89 ± 0.12) with the log β_2 values for substituted pyridines and the fit of this particular data point on the trace in Figure 7 confirms the assignment and rules out any significant π interactions.

Table II. Linear Free Energy Relationships for Substituted Pyridine Complexes of Various Iron Tetraphenylporphyrins

complex	formal oxidn state	solvent	log β_2[a]	Δ log β_2/ ΔpK_a	ρ[b]
$TPPFeL_2$	II	CH_2Cl_2	7.8[c]	0.44[c]	−1.25[d]
$(TPPFeL_2)^+Cl^-$	III	$CHCl_3$	0.2[e]	0.81[e]	
$(TPPFeL_2)^+ClO_4^-$	III	CH_2Cl_2	10.2[c]	1.26[c]	−4.19[d]
$[(TPPFeL)_2N]^+$	?	$EtCl_2$	7.6	0.81	−2.38

[a] Formation constant for the addition of two pyridine molecules. [b] Calculated from plots of log β_2 vs. 2σ. [c] Reference 11. [d] Calculated from results presented in ref 11. [e] Reference 15.

Hammett–Taft relationships were constructed, and a $\rho = -2.38$ was computed. The sign of ρ is identical with that observed for monomeric iron porphyrin complexes and implies that electron-donating substituents on the pyridine facilitate the formation of the complex (see Table II). The magnitude of ρ is intermediate between that observed for Fe(II) and that of Fe(III) porphyrin complexes with identical ligands and further demonstrates the uniqueness of this system with respect to the chemical reactivity vs. valence of the heme iron.

Formation constants for complexation of $TPPFeClO_4$ and TPPFe by pyridine have been reported in CH_2Cl_2 as log β_2^{III} = 10.2 and log β_2^{II} = 7.8, respectively.[11] The value for Fe(II) compares quite favorably with that measured for the dimer (log β_2 = 7.62). However, as shown in Table II, the linear free energy slopes are twice as large for $[(TPPFeL)_2N]^+$ as for monomeric $TPPFeL_2$ and approximate that of $[TPPFeL_2]^+Cl^-$.

Of special note is the magnitude of β_2. Previous measurements of the affinity of TPPFeCl[15] and $TPPFeN_3$[23] for pyridine have yielded values of β_1 = 0.2 and 1.75 M^{-1}, respectively. When these values are compared with that for pyridine addition to $TPPFeClO_4$ (log β_2 = 10.2), a greater than 10^{10} range of β_2 values is observed. The highest values of β_2 are obtained when the Fe(III) monomer was isolated with the weakest coordinating anions. It is tempting to consider the complexation of the formal Fe(IV) atom in the dimer as a monomeric species with $[N^{-II}–Fe^{III}TPP]^-$ as the counterion, in an analogous fashion to Cl^- or N_3^-. On the basis of the Fe(III) monomer trend, one would predict a small formation constant value. Yet, a log β_2 value of 7.62 for pyridine addition is observed. This could imply that Fe(IV) monomers might coordinate axial ligands with a much greater affinity than the Fe(III) counterparts or that an exceptional degree of stability is provided by an $[TPPFe^{IV}–N^{-III}–Fe^{IV}–TPP]^+$ dimer. If the latter is true, then the oxidized μ-oxo dimer should also coordinate axial ligands. Unfortunately, this is not readily verified, as reaction of pyridine with $[(TPPFe)_2O]^+$ or $[(TPPFe)_2O]^{2+}$ species[24] at room temperature results in reduction of the oxidized dimers.

The complexation of the μ-nitrido dimer presented herein is the second report of a six-coordinate dimeric iron porphyrin species.[25] The coordination of the dimer is intriguing when compared to the behavior of the μ-oxo dimer in the presence of similar complexing agents. There is currently no evidence of any axial coordination of the μ-oxo dimer by substituted pyridines. However, Ostfeld[26] has recently reported that the μ-oxo dimer is cleaved by the addition of imidazole in nonaqueous media to form the bis(imidazole) complex of $TPPFe^+$.

(20) Giessner-Prettre, C.; Pullman, B. *J. Theor. Biol.* **1971**, *31*, 287.
(21) Evans, D. F. *J. Chem. Soc.* **1959**, 2003.
(22) Eaton, S. S.; Eaton, G. R. *Inorg. Chem.* **1980**, *19*, 1095.
(23) Adams, K. M.; Rasmussen, P. G.; Scheidt, W. R.; Hatano, K. *Inorg. Chem.* **1979**, *18*, 1892.
(24) Phillippi, M. A.; Goff, H. M. *J. Am. Chem. Soc.* **1979**, *101*, 7641.
(25) Caughey, W. S.; Barlow, C. H.; O'Keeffe, D. H.; O'Toole, M. C. *Ann. N.Y. Acad. Sci.* **1973**, *206*, 296.
(26) Ostfeld, D.; Colfax, J. A. *Inorg. Chem.* **1978**, *17*, 1796.

The stability of the μ-nitrido dimer adducts reported in this study may be attributed, in part, to the increased charge on the bridging N^{3-} atom when compared to that on O^{2-}. Knowledge of the factors responsible for this increased stability is unknown at the present time. Theoretical modeling studies as well as Mössbauer, magnetic, resonance Raman, MCD, and X-ray diffraction experiments are currently under way to more completely characterize bis ligated adducts of iron porphyrin dimers. The results of these investigations will be reported in a subsequent publication.

Acknowledgment. The support of this research from the Robert A. Welch Foundation (Grant E-680) to K.M.K., the National Institutes of Health (Grant GM 25172-02) to K.M.K. and (Grant GM 28831-01) to H.M.G., and the National Science Foundation (Grant CHE-7910305) to H.M.G. is gratefully acknowledged. L.A.B. wishes to thank the Electrochemical Society for the Weston Fellowship. We wish to thank Professor Irwin Cohen for samples of $(TPPFe)_2N$.

Registry No. $(TPPFe)_2N$, 59114-43-1; $[(TPPFe(3,5\text{-dichloropyridine}))_2N]^+$, 78591-76-1; $[(TPPFe(3\text{-cyanopyridine}))_2N]^+$, 78591-77-2; $[(TPPFe(4\text{-cyanopyridine}))_2N]^+$, 78591-78-3; $[(TPPFe(3\text{-chlorpyridinee}))_2N]^+$, 78591-79-4; $[(TPPFe(3\text{-bromopyridine}))_2N]^+$, 78591-80-7; $[(TPPFe(3\text{-acetylpyridine}))_2N]^+$, 78591-81-8; $[(TPPFe(4\text{-acetylpyridine}))_2N]^+$, 78591-82-9; $[(TPPFe(\text{aniline}))_2N]^+$, 78591-83-0; $[(TPPFe(\text{pyridine}))_2N]^+$, 78591-84-1; $[(TPPFe(3\text{-picoline}))_2N]^+$, 78591-85-2; $[(TPPFe(4\text{-picoline}))_2N]^+$, 78591-86-3; $[(TPPFe(3,4\text{-lutidine}))_2N]^+$, 78591-87-4; $[(TPPFe)_2N]^+$, 78591-88-5.

Contribution from the Department of Chemistry, University of California, Davis, California 95616

Indirect Metal–Metal Linkage: Cyclic Ferrocene Complexes with a Second Metal Linked via Remote Phosphine Functionality

NEIL E. SCHORE,* LINDA S. BENNER, and BRUCE E. LABELLE

Received January 27, 1981

The synthesis of the heterodifunctional ligand $(C_6H_5)_2PCH_2Si(CH_3)_2C_5H_4Li$ (**1**) is described, and its utilization as a building block for the preparation of cyclic dinuclear complexes containing dissimilar transition metals is explored. The ferrocene (**2**) derived from **1** is found to coordinate with $Mo(CO)_4$, $Mn(CO)_3Br$, $NiCl_2$, $NiBr_2$, and $Co_2(CO)_6$ fragments through its two phosphine groups. Steric constraints lead exclusively to higher cyclic oligomers in the Mo and Mn complexes and have unusual stereochemical consequences in the Ni systems. The normal chemistry of the Co–Co fragment is unaffected by complexation with diphosphine **2**. An evaluation of the suitability of **1** and related ligands for the construction of different types of heterodinuclear complexes is presented.

Introduction

A most exciting development in the area of transition-metal chemistry as applied to organic synthesis has been the discovery of a number of useful transformations brought about by transition metals operating in pairs. Considerable recent evidence indicates that combinations of "early" and "late" transition metals are particularly interesting in this regard.[1] Our interest lies in the investigation of the synthesis and chemistry of molecules that simultaneously contain both "early" and "late" transition-metal functionality, so that the effects of intramolecularity on variables such as reactivity and stereochemistry may be systematically evaluated.

Our approach to the preparation of compounds containing, for example, a zirconocene-derived moiety indirectly linked to a second metal has involved the development of "heterodifunctional" ligand bridges that allow the specific and sequential attachment of dissimilar transition metals at the two ends.[2] Ideally such a ligand should be readily prepared in high yield, stable to extended storage, and capable of selective, high-yield attachment to the metals in question. The most versatile of the systems we have studied contains a cyclopentadienyl ring linked to a remote phosphine. We recently reported the synthesis of two such ligands and described the first applications of a ligand of this type in indirect metal–metal linkage.[3] The few compounds previously described containing these functional groups have seen only very limited use in transition-metal chemistry[4] and have not been shown to display the attributes most useful for this purpose.

We report here full details of the synthesis of the ligand [[dimethyl((diphenylphosphino)methyl)silyl]cyclopentadienyl]lithium (**1**) and describe the preparation of a number of complexes of its ferrocene derivative (**2**) with second

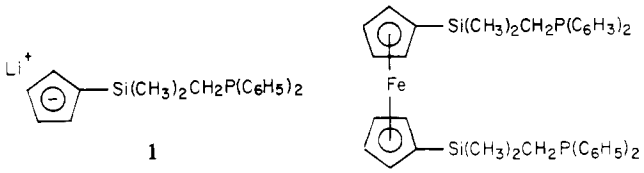

1 **2**

metal centers. The properties of these compounds are described and compared with known systems from the point of view of ferrocene **2** as a structural model for analogues derived from metallocenes containing metals other than iron. On the basis of these results, the general utility of ligand **1** for the preparation of the desired bimetallic systems is critically evaluated.

(1) E.g.: (a) Dayrit, F. M.; Gladkowski, D. E.; Schwartz, J. *J. Am. Chem. Soc.* **1980**, *102*, 3976. (b) Negishi, E.; Kukado, N. O.; King, A. O.; Van Horn, D. E.; Spiegel, B. I. *Ibid.* **1978**, *100*, 2254. (c) Hansen, R. T.; Carr, D. B.; Schwartz, J. *Ibid.* **1978**, *100*, 2244. (d) Loots, M. J.; Schwartz, J. *Tetrahedron Lett.* **1978**, 4381; *J. Am. Chem. Soc.* **1977**, *99*, 8045. (e) Negishi, E.; Van Horn, D. J. *Ibid.* **1977**, *99*, 3168. Involving nontransition metals, see: (f) Carr, D. B.; Schwartz, J. *Ibid.* **1979**, *101*, 3521. (g) Van Horn, D. E.; Negishi, E. *Ibid.* **1978**, *100*, 2252. (h) King, A. O.; Negishi, E.; Villani, F. J.; Silveira, A. *J. Org. Chem.* **1978**, *43*, 358. (i) Giacomelli, G.; Lardicci, L. *Tetrahedron Lett.* **1978**, 2831.

(2) Schore, N. E.; Hope, H. *J. Am. Chem. Soc.* **1980**, *102*, 4251.

(3) (a) Schore, N. E. *J. Am. Chem. Soc.* **1979**, *101*, 7410. (b) Schore, N. E.; Sundar, S. *J. Organomet. Chem.* **1980**, *184*, C44.

(4) (a) Mathey, F.; Lampin, J.-P. *Tetrahedron* **1975**, *31*, 2685. (b) Mathey, F.; Lampin, J.-P. *J. Organomet. Chem.* **1977**, *128*, 297. (c) Charrier, C.; Mathey, F. *Tetrahedron Lett.* **1978**, 2407. (d) Charrier, C.; Mathey, F. *J. Organomet. Chem.* **1979**, *170*, C41.

0020-1669/81/1320-3200$01.25/0